Energy 79 (2015) 117–126

Contents lists available at ScienceDirect

Energy

journal homepage: www.elsevier.com/locate/energy

Parametric assessment of a low-swirl burner using the exergy analysis

M.E. Feyz*, S.I. Pishbin, M. Ghazikhani, S.M.R. Modarres Razavi

Department of Mechanical Engineering, Ferdowsi University of Mashhad, Mashhad 91775-1111, Iran

ARTICLE INFO

Article history:
Received 1 March 2014
Received in revised form
1 September 2014
Accepted 26 October 2014
Available online 5 December 2014

Keywords:
Low swirl burner
Exergy destruction
Premixed combustion
Flame regime

ABSTRACT

The performance of a low-swirl burner (LSB) operating on natural gas is experimentally examined. Due to the unique features of the LSB, many studies have been previously conducted to specify the design limits. However, this study aims to employ the exergy analysis to highlight specific design preferences within the combustion stability ranges. The assessed parameters in this work are fuel–air equivalence ratio, burner recess length, swirl number and thermal input rate. Based on the stream characteristics, two main flame regimes are distinguished. Tracing of entropy generation reveals the significance of fuel exergy destruction in the attached flame regime in comparison with the lifted flame. Also it is declared that for all the examined recess lengths, the irreversibility ratio depicts the same minimum value when the burner is operating at $\Phi = 0.68$. Interestingly, unlike the ordinary diffusion flames, decreasing the swirl number of LSB slightly contributes to the reduction of irreversibility. In the present combustion system on the average basis, only 34.5% of total fuel exergy is destroyed which marks the merits of LSB premixed combustion over swirl-induced diffusion burners.

1. Introduction

During the recent years, strict emission standards in power generation and industrial applications urged the utilization of lean, premixed combustion as a desirable clean combustion technology. This combustion mode exhibits low NO_x and CO emissions without steam injection. Thus, lean-premixed combustion is the basis of the current dry low emissions (DLE) gas turbine combustion systems. When operating on natural gas, CO and NO_x emissions can drop even below 50 and 25 ppm, respectively (corrected to 15% O_2) with the aid of the DLE combustion system [1–3].

Although lean-premixed combustion exhibits several merits in terms of efficiency and emissions, the premixed combustion stability is quite challenging issue due to the flame structure and flame propagation velocity. Swirl-stabilized combustion is widely used as a flame stabilization technique in premixed combustions [4,5]. It promotes the flame stability via creating recirculation zones in the flow field that transport heat and radicals of the products into the reactants which can enhance the flame propagation velocity. Nevertheless, the circulation zones provide the hot spots with high residence time that act as thermal NO_x generators [3].

In order to terminate the drawbacks of high swirl stabilization, researches in the last decade introduced a new technology which reduces the need for recirculation zones in order to stabilize premixed flames. Originally developed at the Lawrence Berkeley National Laboratory, Low Swirl Combustion (LSC) is identified as one of the most promising strategies for premixed combustion stabilization. The low swirl burner (LSB) was initially proposed by Chan et al. [6] and mainly developed by Cheng and others [7–9]. Low-swirl combustion has been commercialized for industrial process heaters and is being employed in gas turbines [10].

The main operating principle of LSB lies within the propagating nature of turbulent premixed flames. In LSBs, the “standing flame front” is accomplished by producing weak swirl which leads to a divergent downstream flow. Original study [11] clarified that unlike the flames stabilized by high amounts of swirl, LSB flames do not rely on flow recirculation for stabilization. The main feature of the LSB is the unique design of swirl injector (Fig. 1), which provides slight swirl flow and facilitates downstream divergent flow where the flame front can be settled.

Several projects have been pursued to adapt LSB to industrial and commercial heaters. Accordingly, the efforts have been made to offer design instructions by which the limits of geometric parameters are defined [12,7].

With recent comprehensive studies on the stability mechanisms and structure of LSB [13], this technology still lacks attempts for further Thermodynamics studies in order to have a better understanding of its nature. In the past two decades, second law of Thermodynamics introduced an effective concept for evaluation of the thermal system deficiencies named “Exergy/Availability” or

* Corresponding author. Tel.: +98 915 307 5611; fax: +98 513 7636425.
E-mail addresses: mo.feyz@alumni.um.ac.ir, m.e.feyz@gmail.com (M.E. Feyz).

http://dx.doi.org/10.1016/j.energy.2014.10.074
0360-5442/

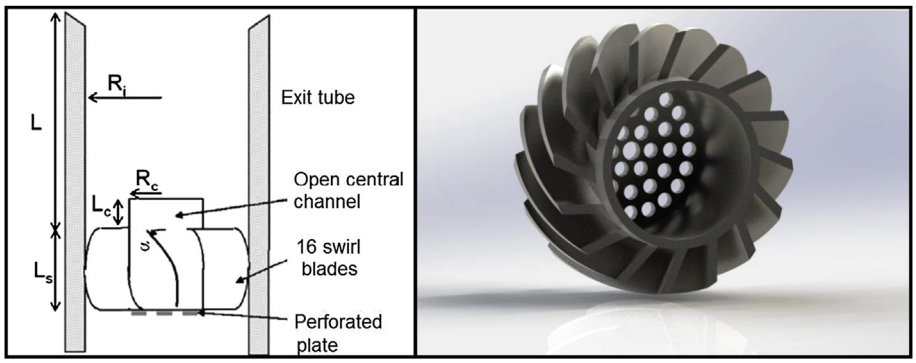

Fig. 1. The schematic diagram of LSB swirl injector; inner radius (R_i), core radius (R_c), recess length (L), swirl length (L_s), channel length (L_c), blade angel (α).

maximum attainable work [14]. In the field of power generation, it is known fact that combustion is always associated with considerable exergy destruction due to the complexity of the process [15].

Generally, the well-known Gouy-Stodola theorem establishes the connection between the lost exergy or irreversibility and the entropy generation [16]. Destruction of fuel chemical exergy in multicomponent reacting flows occurs through different sources of entropy generation in combustion phenomena [15]. Major causes of the entropy generation during combustion are introduced in a study by Dunbar and Lior [17] as chemical reaction, heat transfer due to temperature differences, species mass transport and viscous dissipation. Accordingly, Dunbar and Lior introduced heat transfer as the main source of entropy generation.

The dominant entropy generation mechanism seems to be different in premixed and non-premixed flames. In the work of Nishida et al. [18], the comparison is made between premixed and diffusion flame in order to identify the influence magnitude of each entropy process. Also, the operating parameters such as air–fuel ratio and inlet temperature on the entropy generation in a typical premixed flame are studied. They declared that the chemical reaction is the dominant factor of entropy generation in premixed combustion whereas for diffusion flames, it is heat transfer that comprises a major part of entropy generation. They also stated that for methane combustion, the total entropy generation reduces with increasing the equivalence ratio from 0.7 to 1. This is believed to be caused by the effect of equivalence ratio on the combustion temperature and the reaction zone thickness. The overall exergy analysis also confirms the superiority of stoichiometric combustion on reducing the combustion internal irreversibility [19].

There may be a contrasting point while comparing the observations of Dunbar and Lior [17] with the ones of Nishida et al. [18]. Even though, Dunbar and Lior introduced heat exchange as the dominant entropy generation process in premixed flames, Nishida et al. attributes the major entropy generation to the chemical reactions. The reason within the conclusion of Nishida et al. may rely on their assumption of reaction zone, which keeps the temperature gradients outside of the flame extremely low.

Most of the combustion applications involve turbulent reacting flows. The turbulent flow exhibits entropy generation due to extracting energy from the main stream to maintain its fluctuating nature. Stanciu et al. [20] split the sources of fuel exergy destruction into mean and turbulent parts for heat/mass transfer, chemical and viscous components. It turned out that the turbulent viscous, thermal and diffusion entropy are considerably greater than those generated in the mean motion field. In a practical investigation, Yapici et al. [21] conducted a numerical simulation for turbulent diffusion combustion of CH_4-air in which the inlet air passes through swirl injector and enters as co-flow with fuel. The effects of fuel–air equivalence ratio and swirl number are exclusively examined on the rate of entropy generation in the system. The results imply that increasing the swirl number in particular conditions can restrict the entropy generation. Moreover, the investigation of Makhanlall and Liu [22] showed the importance of entropy generation due to radiation for macro-scale combustion systems, while radiation entropy generation is usually neglected in micro-scale combustions [23].

Utilization of diffusion combustion in industries is widespread due to its simplicity and higher safety. Applying the exergy balance to the common applications of diffusion combustion shows the irreversibility values ranging from 44 to 71% of total fuel exergy. The irreversibility production is lower in gaseous fuels and is higher in liquid and solid fuels, respectively [24–26].

The limited number of exergy studies on the premixed turbulent flames usually has not vastly succeeded in providing a practical insight about the effective irreversibility production sources. The introduction of low swirl combustion, as the leading stability mechanism of the modern gas turbines, necessitates the investigation of this technology via exergy approach. In this study, LSB combustion as a perfect example of propagating turbulent premixed flame is examined experimentally and the effects of design and operational parameters on its exergetic performance are studied. The results of the following investigation can provide a better insight for selection of design parameters in a manner that exergy destruction meets its minimum.

2. Test rig and experimental procedure

The main component of the LSB is a swirl injector which is responsible for flame stability. The swirler supplies the air–fuel mixture through two passages: an outer annular region with swirling vanes and a central channel that permits a fraction of the flow to remain unswirled (Fig. 1). In order to control the flow rate allocated to each passage, a perforated plate is attached to the central channel.

The aerodynamic uniqueness of the LSB swirler provides a highly turbulent flow with slight swirl that can promote the divergent flow downstream of the burner exit and avoids the formation of recirculation zone. The swirl number for LSB practice is defined as:

$$S = \frac{2}{3}\tan\alpha \frac{1-R^3}{1-R^2+\left[m^2\left(\frac{1}{R^2}-1\right)^2\right]R^2} \quad (1)$$

where from Fig. 1, α is the angle of 16 vanes mounted around the central channel and $R = R_c/R_i$. The parameter $m = m_c/m_s$ is the ratio

of the unswirled portion, m_c, and the swirled, m_s, flows. This ratio is inversely related to the blockage caused by the perforated plate and can be determined simply by the use of standard flow pressure drop procedure. In the present study, the burner has annular and core radius of $R_i = 34.5$ mm and $R_c = 22.5$ mm, respectively, with the ratio of $R = 0.64$. The channel and swirl lengths are as $L_c = 6$ mm and $L_s = 28$ mm. Also, the vane angles are adjusted as $\alpha = 41$. During the experimental procedure, the attempt is made to examine the effect of recess length (L), swirl number (S), mixture equivalence ratio (Φ) and thermal input rate on the exergy performance. Mixture equivalence ratio is defined as follows:

$$\phi = \frac{\left(\dot{m}_f/\dot{m}_{air}\right)_{Actual}}{\left(\dot{m}_f/\dot{m}_{air}\right)_{Stoichiometric}} \quad (2)$$

Table 1 indicates the tested configurations of the burner. For swirl of $S = 0.56$, two different recess lengths are implemented (Conf. I and II). According to Eq. (1) based on the blockage ratio of the central channel, different swirl numbers can be produced. Therefore, $S = 0.5$ is produced by varying the blockage ratio (Conf. III).

All the cases are operating on natural gas with the composition presented in Table 2. Due to the high fraction of Methane in the used gas composition, the dynamic behavior of premixed Methane/air flames can be expected.

For the cases I and II, at the constant fuel rate of ≅1.1 g/s, the mixture equivalence ratio is varied (Φ = 0.61, 0.68, 0.78, 0.88). However, it should be noticed that for the purpose of changing equivalence ratio, the combustion air flow rate was controlled via the needle valve. Hence, changing the mixture equivalence ratio is associated with the change of the bulk velocity exiting the burner. The correlation of mixture bulk velocity and equivalence ratio is illustrated in Fig. 2.

In order to investigate the impact of thermal input rate on exergy performance, for configuration III the burner exit velocity at constant equivalence ratio of $\Phi = 0.88$ is varied to evaluate the response of the system to the different heating capacities (35, 56 and 66 kW).

The LSB is horizontally mounted to a cylindrical combustion chamber with 45 cm and 150 cm of diameter and length, respectively. The chamber body is not insulated so that the heat exchange can freely occur with the surroundings.

Fig. 3 shows the schematic presentation of the test rig and measuring facilities. As it is shown, the air supplied by the high-pressure blower and natural gas separately enter the mixing tube and the homogenous mixture is delivered to the burner inlet. The volumetric flow rate of air and fuel are measured by the turbine and bellows meters, respectively. Having the corresponding pressure and temperature, the mass flows can be calculated by treating air and natural gas as ideal gases. A total number of the 9 ports are mounted along the combustor wall by various spacing intervals in order to measure axial and radial temperatures of gas by an S-type thermocouple. The first port is located 5 cm downstream of the burner exit. The temperature of the combustor walls is recorded by infrared thermometer, BE900.

Table 1
Test configurations of the LSB.

LSB configuration	Recess length L (mm)	Blockage (%)	$m = m_c/m_s$	Swirl no.
I	$2R_i = 69$	61	0.43	0.56
II	$3R_i = 104$	61	0.43	0.56
III	$2R_i = 69$	41	0.55	0.5

Table 2
Natural gas composition.

Gas formula	Mole fraction (%)
CH_4	98.231
C_2H_6	0.551
C_3H_8	0.052
i-C_4H_{10}	0.041
n-C_4H_{10}	0.033
i-C_5H_{12}	0.022
n-C_5H_{12}	0.026
$C_6H_{14}^+$	0.039
CO_2	0.509
N_2	0.496
H_2S	3.00 ppm

Molecular weight = 16.42, specific gravity = 0.5671.
LHV (kJ/kg) = 49,366.

The exhaust gases exit the combustor from a 15 cm circular opening located at the end of the chamber to prevent the entrainment of ambient air into the combustion products. The combustion product species (O_2, CO, CO_2, NO, NO_2, Unburned hydrocarbons) are measured on dry basis using TESTO XL-350 gas analyzer. Table 3 displays the accuracy and uncertainties of the measuring devices. For all the test points, the burner-combustor began operating for 30 min to achieve steady thermal conditions and then data acquisition started. In order to determine the repeatability of the testing process, random tests are conducted in one month interval. The average deviation of combustor wall temperature measurements within the interval time was 3%, which has not influential figure in the results of exergy calculations.

3. Second law mathematical model

For semi-steady state systems, the second law analysis can begin with applying the overall availability/irreversibility balance.

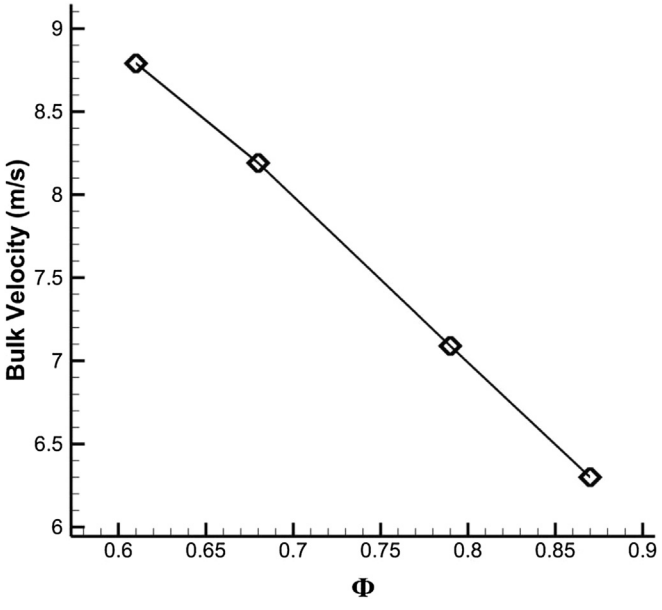

Fig. 2. Variation of the corresponding velocities with mixture equivalence ratios.

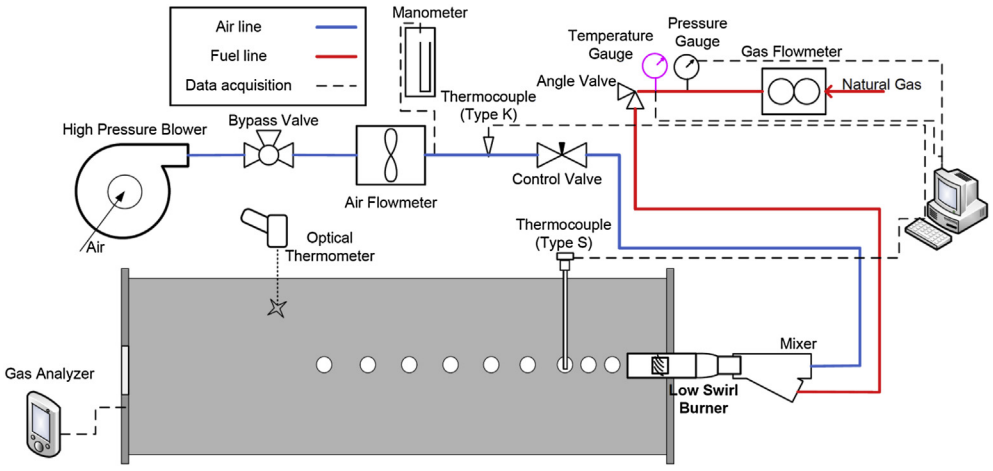

Fig. 3. Schematic view of the test rig and measuring facilities.

3.1. General availability balance equation

For an open control volume experiencing energy and mass exchange with the surrounding environment, the following equation for the change of availability on a time basis exists [27]:

$$\int \frac{dA_{cv}}{dt}ds = \int_j \dot{Q}_j\left(1-\frac{T_0}{T_j}\right)ds - \left(W_{cv} - P_0\frac{dV_{cv}}{dt}\right) + \sum_i (\dot{n}_i\psi_i)_{in} - \sum_i (\dot{n}_i\psi_i)_{out} - \dot{I}_{cv} \quad (3)$$

In the above-stated terms, dA_{cv}/dt is the rate of availability change by time in the system which is nearly equal to zero for the present work. Also the term $W_{cv} - P_0\, dV_{cv}/dt$ is equal to zero due to none shaft work transfer and constant occupied volume.

$\int \dot{Q}_j(1 - T_o/T_j)ds$ represents the availability associated with heat transfer from the combustor walls where T_j is the temperature of the boundary and $\dot{Q}_j$ is the rate of heat transfer to or from the working medium over a differential area. For the present investigation, T_j is considered as the temperature of the combustor outer wall. Also, T_o is the dead-state temperature. The thermo-chemical values of the taken dead-state are presented in Table 4.

Calculation of the dissipated heat from the combustor walls to the surrounding is done by dividing the wall into eight thermal regions. The average temperature of each thermal region was measured which enables one to predict the convective and radiative heat transfer.

Heat losses from the non-insulated wall to the ambient are given by:

$$\dot{Q}_j = A \times \left[h_{conv}(T_j - T_{sur}) + h_r(T_j - T_{sur})\right] \quad (4)$$

where h_{conv} and h_r represent the convective and radiative heat transfer coefficients, respectively. The free convection heat transfer occurs on the horizontal cylinder of the combustor and on the vertical sidewalls. The Nusselt number (Nu) can be obtained for horizontal cylinder with diameter D, via the semi-empirical Eq. (5) [28]:

Table 3
Error and uncertainties of measuring instruments.

Device	Specie	Unit	Resolutions	Absolute error	Deviation from the reference composition
Gas analyzer Testo XL-350	O_2	volume %	0.01	0.008	±2%
	CO_2	volume %	0.01	0.008	
	H_2	ppm	1	–	
	UHC	ppm	1	–	
	CO	ppm	1	10	
	NO_2	ppm	0.1	5	
	NO	ppm	1	10	
	NO_x	ppm	1	10	
	Type	*Unit*	*Reference temperature*	*Absolute error*	*Uncertainty*
Thermocouple and indicator	S (SG-T-01)	°C	800.7	−0.70	±2.10 °C
			1000.5	−0.50	
			1200.8	−0.80	
	Infrared (BE900)	°C	0–900	1.5 (as $\varepsilon \to 1$)	±6.45 °C
	Type	*Standard flow range*		*Resolutions*	*Standard accuracy*
Flow counter	Air turbine meter (Vemmtec-DN80)	Q_{max} (m^3/h) = 160	Q_{min} (m^3/h) = 6.4	0.1 (m^3/h)	±2% for Q_{min} to 0.2 Q_{max} ±1% for 0.2 Q_{max} to Q_{max}
	Gas bellow meter (GS-79-016A)	Q_{max} (m^3/h) = 25	Q_{min} (m^3/h) = 0.16	0.01 (m^3/h)	±3% for Q_{min} to $2Q_{min}$ ±2% for $2Q_{min}$ to Q_{max}

Table 4
The Thermochemical values of the standard dead-state.

$T_0 = 298.15$ K, $P_0 = 0.101325$ MPa	
Substance	Mole fraction (%)
N_2	78.09
O_2	20.95
CO_2	0.03
Other	0.93
H_2O	Zero

$$\overline{Nu}_D = \frac{hD}{K} = \left\{0.6 + \frac{0.387Ra_D^{1/6}}{\left[1+(0.559/Pr)^{9/16}\right]^{8/27}}\right\}^2, \quad Ra_D = \frac{g\beta(T_s - T_\infty)D^3}{\vartheta\alpha} \quad \text{and} \quad Pr = \frac{\nu}{\alpha} \tag{5}$$

And for the vertical plates with the length, L, *at* the two ends of the combustor, Nu is calculated by Eq. (6) [28]:

$$\overline{Nu}_L = \frac{hL}{K} = \left\{0.825 + \frac{0.387Ra_L^{1/6}}{\left[1+(0.492/Pr)^{9/16}\right]^{8/27}}\right\}^2 \tag{6}$$

All the gas properties at the film temperature are selected at $T_f = 650$ K. Also the radiative heat convection coefficient is obtained through the following approximation where the emissivity coefficient of the rusted steel is almost known to be $\varepsilon = 0.85$.

$$h_r \equiv \varepsilon\sigma(T_j + T_{sur})\left(T_j^2 + T_{sur}^2\right) \tag{7}$$

The flow availability in multi-component reacting systems consists of thermomechanical and chemical components. In Eq. (3), ψ_{in}, ψ_{out} represent the inlet and outlet flow exergy on the molar basis, respectively, which can be stated as [14]:

$$\sum_i n_i\psi_i = n_i\left(\psi_i^{tm} + \psi_i^{ch}\right) \tag{8}$$

With negligible kinetic energy and considering $P = P_0$, the thermo-mechanical flow exergy of the ith specie on a molar basis is defined as:

$$\psi_i^{tm} = (h - h_0)_i - T_0(s - s_0)_i \tag{9}$$

where h_0 and s_0 represent the enthalpy and entropy of the ith specie at the dead-state temperature and pressure.

Also, the chemical exergy of the ith specie in a mixture is defined as follows [29]:

$$\psi_i^{ch} = \varepsilon_i^0 + \tilde{R}T_0 \ln Y_i \tag{10}$$

where ε_i^0 is the standard chemical exergy of the ith specie in the inlet or exhaust mixtures, $\tilde{R}$ is the universal gas constant and Y_i is the mole fraction of the ith specie. Due to the fact that Eq. (10) generally applies to all the chemical species including the fuel, it removes the need for calculation of fuel exergy individually.

Then, the irreversibility ratio of the burner-combustor is written as:

$$Irr = \frac{\dot{I}}{\dot{n}_f\psi_f} \tag{11}$$

In Eqs. (3) and (11), $\dot{I}$ is the rate of irreversibility production inside the control volume due to heat and mass transport, chemical reaction, radiation and viscous friction. In fact, since the boundary of the control volume in the present study is limited to the combustor walls and does not encompass the surrounding, the term "irreversibility" used in this paper refers to the internal irreversibilities of the system.

3.2. Equations for entropy generation in combustion

In any thermal-reacting system, the entropy is generated by several sources. The total entropy generation in combustion can be mainly attributed to the following sources; viscous friction, heat and mass exchange, chemical reaction and thermal radiation.

Viscous entropy generation is caused by viscous shear stress. S_f indicates the volumetric local entropy generation due to viscous friction and can be described as [21]:

$$S_f = \frac{\mu}{T}\Phi_v \tag{12}$$

where μ is the effective mixture viscosity and Φ_v is the viscous dissipation term which in axi-symmetrical geometry can be stated as [21]:

$$\Phi_v = 2\left[\left(\frac{\partial u}{\partial x}\right)^2 + \left(\frac{\partial v}{\partial r}\right)^2 + \left(\frac{v}{r}\right)^2\right] + \left(\frac{\partial u}{\partial r} + \frac{\partial v}{\partial x}\right)^2 \tag{13}$$

Entropy generation due to heat exchange is the other important source of entropy generation which can be formulated as [21]:

$$S_{th} = \frac{k}{T^2}(\nabla T)^2 = \frac{k}{T^2}\left[\left(\frac{\partial T}{\partial x}\right)^2 + \left(\frac{\partial T}{\partial r}\right)^2\right] \tag{14}$$

where k is the effective thermal conductivity of the gas mixture.

The entropy generation associated with the chemical reaction and radiation are also characterized in literature [22]; even though they are not addressed in this study.

4. Results and discussion

4.1. Overview of the thermal impacts

The flame geometry and thermal characteristics are believed to have a major impact on the exergetic behavior of combustion [30]. Hence, the thermal features of LSB flame need to be studied prior to applying the exergy analysis.

Running the LSB in open environment experiments demonstrated two distinguished flame regimes; lifted and attached flames (Fig. 4). The regime under which combustion is occurring is mainly controlled by the downstream flow field in addition to the fuel content of the reactants. The thermo-fluid features of the unburnt gases determine the suitable region for the flame brush to be

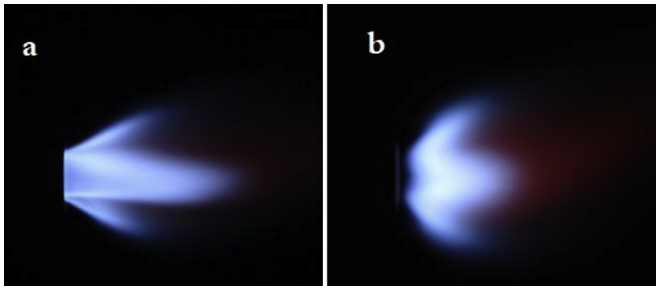

Fig. 4. Dominant flame regimes of the present LSB; (a) attached flame, (b) lifted flame.

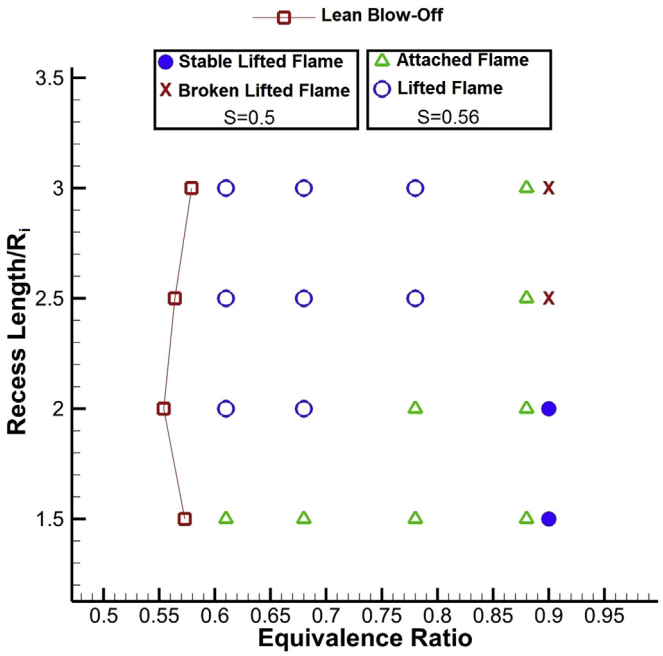

Fig. 5. Flame pattern regime diagram of the present LSB.

settled. As depicted in Fig. 4, the flame in the attached regime is stabilized at the exit port of the burner and it exhibits a concentrated thermal region near the axis of the LSB; while the lifted flame regime provides a detached reaction zone with an extended flame brush. Accordingly, one would expect more thermally distributed region in lifted regime in comparison with the attached regime.

The design parameters of LSB (recess length and swirl number) as well as fuel–air equivalence ratio are influencing the flame regime. The formers affect the regional flow field and the latter determines the flame propagation speed. Fig. 5, shows the various flame regimes that may occur due to changing the design and operational parameters.

Shifting the flame regime by increasing the recess length (L) is mainly due to the variation of burner exit flow field. By increasing the recess distance, the swirling momentum of the flow gradually dissipates which leads to increasing the axial momentum. Hence, the divergent region downstream of the burner exit is weakened and provides a lifted flame. Reducing the swirl number is also having a similar effect on the flow field. However, the combustion exhibits rather high instability with $S = 0.5$ in comparison with $S = 0.56$ which restricts the possibility of LSB operation in equivalence ratios below $\Phi = 0.88$ with $S = 0.5$.

4.2. Exergy analysis

The process diagram of the combustion system is presented in Fig. 6. As shown, the investigated control volume accommodates air–fuel mixer, LSB and the combustor to the extent that it does not involve the surrounding.

The exergy performance of the low swirl combustion rationally must be influenced by reactants condition and design characteristics. Each part is examined separately in the Sections 4.2.1 and 4.2.2. Besides, the effect of thermal input rate on the exergy destruction of low swirl combustion will be discussed in Section 4.2.3.

4.2.1. Effect of fuel–air mixture

For various fuel–air equivalence ratios, the thermal properties and exergy terms of the indicated fluxes crossing the boundary of control volume are presented in Table 5. Table 5 depicts the flow and heat condition of the combustion system as well as the corresponding exergy terms for different fuel–air mixtures at $L = 2R_i$ and $S = 0.56$. From the energy viewpoint, it is observed that the variations of heat loss and exhaust energy changes meaningfully by changing the reactant equivalence ratio.

In Table 5, one can observe that by increasing Φ, the heat loss from the combustor body decreases while the energy content of the exhaust gases increases. As previously addressed in Fig. 5, at $L = 2R_i$ the LSB combustion during $\Phi = 0.61$ and 0.68 demonstrates lifted flame regime while at $\Phi = 0.78$ and 0.81 the attached flame regime is dominant. Since in the lifted flames temperature distribution is widespread, it causes relatively more heat transfer to the walls and less exhaust losses when the LSB is operating in low equivalence ratios.

Similarly, as the flame regime changes from lifted flame ($\Phi = 0.61$ and 0.68) to the attached regime at higher equivalence ratios, the exergy transfer via exhaust gases and body heat exchange experiences a sudden change.

Fig. 7 displays the contribution of each process in total exergy balance of the combustion system for various fuel–air equivalence ratios. The results are shown as the percentage of the fuel exergy. As Fig. 7 shows, the exergy associated with heat transfer from the walls has the greatest allocation of fuel exergy with the 50.5 percent on the average basis. Then, the irreversibility and the exhaust exergy ratio comprise the other fuel exergy losses with average 35.5 and 13.9 percent, respectively. Interestingly, the irreversibility ratio in the present premixed combustion is considerably lower than other values reported in the literature for traditional diffusion combustion systems [24–26].

In Fig. 7, it is observed that as $\Phi = 0.68$ goes to $\Phi = 0.78$, there is a sudden decline in the heat exergy ratio by 11.7%, relatively. On the opposite side, a sudden rise of relatively 14% is occurring in the exhaust exergy ratio. This behavior is mainly lies within the effect of flame regime on the exergy distribution in the entire system. In

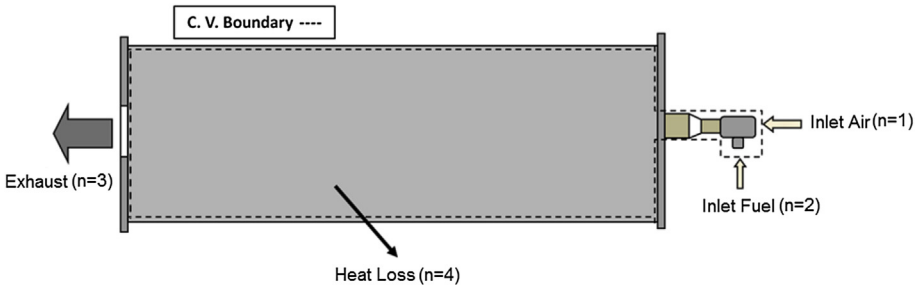

Fig. 6. The designated control volume under study.

Table 5
The thermal properties of the heat/mass fluxes crossing the control volume boundary ($L = 2R_i$, $S = 0.56$).

Φ	n	Temperature T (°C)	Gage pressure P (kPa)	Entropy s (kJ/kmol K)	Energy e (kJ/kmol)	Molar flow rate $\dot{n}$ (kmol/h)	Heat loss $\dot{Q}$ (kW)	Exergy value (kW)
0.61	1	34	3.72	0.850	257.07	3.913		0.00365
	2	25.5	2.43	1.062	318.5	0.256		59.448
	3	444	≅0	27.857	4974.8	4.255	5.87	7.736
	4						52.09	31.259
0.68	1	46	3.81	1.968	606.30	3.495		0.0189
	2	30	2.43	2.473	757.126	0.252		58.565
	3	467	≅0	28.991	5548.3	3.780	5.82	7.662
	4						51.60	31.290
0.78	1	49	3.91	2.250	696.645	2.955		0.0211
	2	32	2.43	2.832	871.707	0.247		57.509
	3	566	≅0	33.465	10,514.9	3.246	9.48	8.591
	4						46.90	27.141
0.88	1	49	4.02	2.250	693.73	2.622		0.0185
	2	30	2.43	2.821	868.99	0.244		56.619
	3	579	≅0	34.158	10,624.4	2.894	8.54	8.195
	4						46.91	27.355

Enthalpy and entropy are calculated with respect to the dead-state reference.
For fuel stream, the sensible enthalpy is only addressed in the table.

lower equivalence ratios, as the lifted flame has a more extended surface, the greater part of the fuel exergy is convected to the combustor walls while the lower fuel availability is exiting through the hot exhaust products. This manner is inversely occurring during higher equivalence ratios where the attached flame regime is dominant.

Fig. 7 clearly reflects the influence of the flame regime in the variation of irreversibility ratio. One can observe that from $\Phi = 0.68$ to 0.78, the irreversibility ratio experiences almost 13.3 percent rise comparatively. In fact, the reason of this significant change originates from the influence of the flame regime on thermal distribution inside the combustion chamber. Obviously, the lifted flames which occur at Φ lower than 0.68 express better performance in terms of exergy. However, within each flame regime, the increase of Φ lowers the irreversibility ratio.

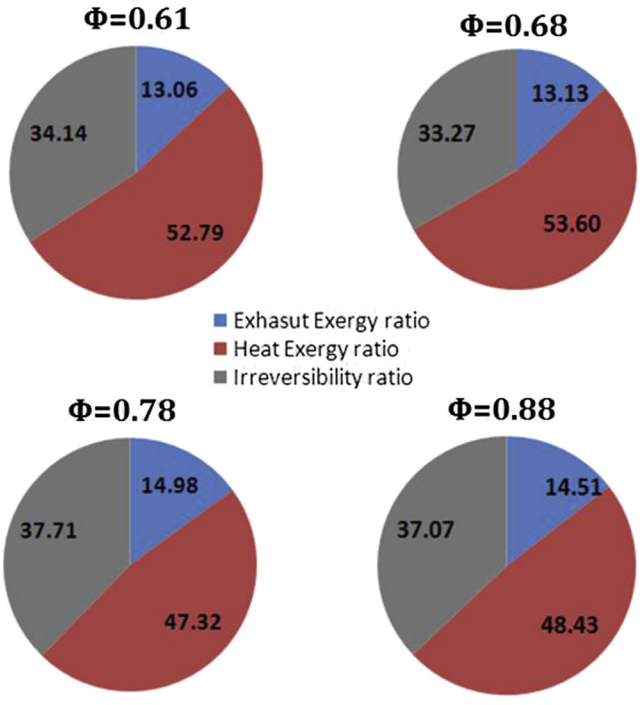

Fig. 7. Effect of equivalence ratio on exergy balance of combustion system ($L = 2R_i$, $S = 0.56$).

In order to clarify the effect of flame regime on the rate of exergy destruction, the temperature distribution for two distinguished flame regimes, i.e. attached and lifted flame, on the mid-plane of the combustor is illustrated (Fig. 8a and c). The temperature contours presented in Fig. 8 are obtained from the experimental data, which are interpolated using Triangle Cubic Interpolation method. It is perceived from the former studies [17,31] that in the premixed combustion, entropy generation due to heat transfer within the combustion chamber is the most dominant process or at least is of high influence. According to the Eq. (14), the rate of thermal entropy generation is directly dependent to the $(\nabla T/T)^2$ which indicates the intensity of local non-dimensional temperature gradients. Therefore, for characterizing the distribution of thermal entropy generation, the $(\nabla T/T)^2$ distribution is calculated for the mid-plane of the combustor to show the effect of flame regime on this parameter as the indication of thermal entropy generation.

Fig. 8b and d depicts the variations of $(\nabla T/T)^2$ across the 2-D plane within the combustor. Apparently, the intensity of local temperature gradients is quite strong in the attached flames. This can be due to the fact that in the attached flame regime, the high temperature is greatly concentrated around the axis while at lifted flames, the temperature is widely spread along the combustor radius. Hence, higher rate of irreversibility would be expected in attached flames compared to the lifted flames in general overview.

4.2.2. Effect of design characteristics

The characteristic parameters of LSB design can significantly affect the flow pattern of the reactants. Hence, it is expected that by changing flow field, the burner performs differently in terms of exergy. The recess length and swirl number are two crucial factors in flame stability mechanism in LSBs. They both act in parallel to maintain the divergent downstream flow and stream uniformity.

Fig. 9 demonstrates the comparison of heat and exhaust exergy for two different recess lengths. As seen, the LSB with longer recess length shows better exergy transfer via heat exchange to the walls. Increasing recess length in higher equivalence ratios can cause relatively 14.8 percent improvement in the exergy transfer by heat exchange. For exergy transferring by exhaust gases, it is observed that in rich mixtures ($\Phi = 0.78$ and 0.88) the exhaust exergy tends to be lower in recess of $L = 3R_i$ in comparison with $L = 2R_i$ while it is slightly higher for lower equivalence ratios ($\Phi = 0.61$ and 0.68).

The reason that exergetic performance of the combustion is affected by the recess length originates from the effect of recess on

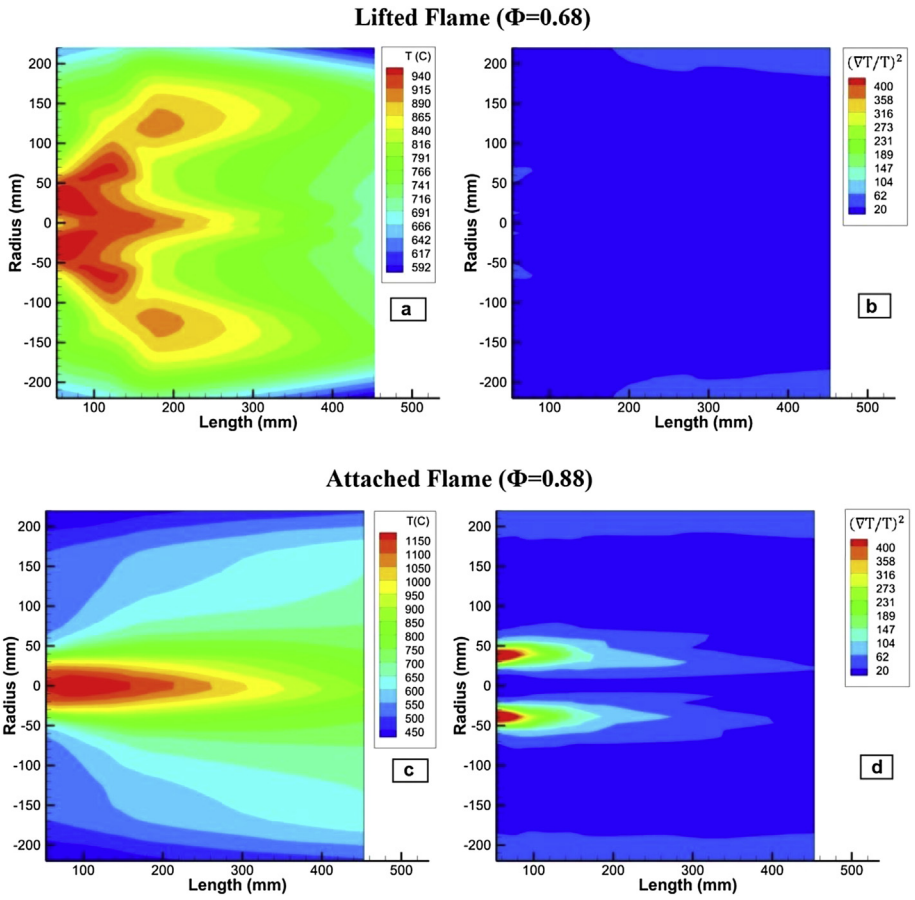

Fig. 8. Temperature distributions (a, c) and normalized temperature gradients (b, d) of lifted and attached flames ($L = 2R_i$, $S = 0.56$).

flame shape and effective heat transfer area. In higher recess lengths, the flame surface is more extended which causes better heat transfer from the flame to the walls. Hence, one can generally expect higher heat transfer exergy by increasing the recess distance. Accordingly, the exhaust exergy is influenced by varying the recess length in a manner that it covers the balance between heat transfer exergy and irreversibility. However, it must be taken into consideration that the flame stability studies put a limit to the extent that recess length can be increased which is roughly $L = 3R_i$ [7].

The change of system irreversibility in various fuel–air equivalence ratios is depicted in Fig. 10 and the comparison is made between two different recess lengths. In a general observation, it is clear that the exergy destructions due to combustion irreversibilities declines relatively 5.6 percent averagely for $L = 3R_i$ comparing to $L = 2R_i$. The reason lies within the suitable temperature distribution of the combustion when the burner is operating with higher recess length. In the other words, as the recess length increases, the flame brush spreads further in the chamber that can provide more thermally uniform region. It restricts the amount of entropy generation that mainly occurs by strong temperature gradients around the axis.

The interesting observation in Fig. 10 is despite the fact that combustion generally has the lowest exergy destruction near stoichiometric conditions [19], in the present LSB the lowest exergy destruction occurs in the lean mixture with $\Phi = 0.68$. Although in lean combustion temperature is lower, the uniform flame brush of LSB limits the severe thermal entropy generation which leads to an overall reduction of irreversibility production. The accumulative

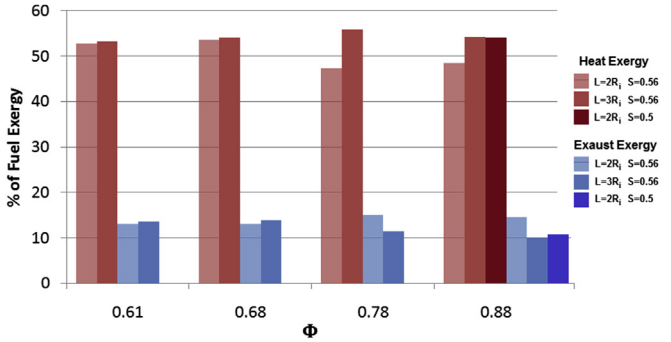

Fig. 9. Comparison of heat and exhaust exergy for recess and swirl variation.

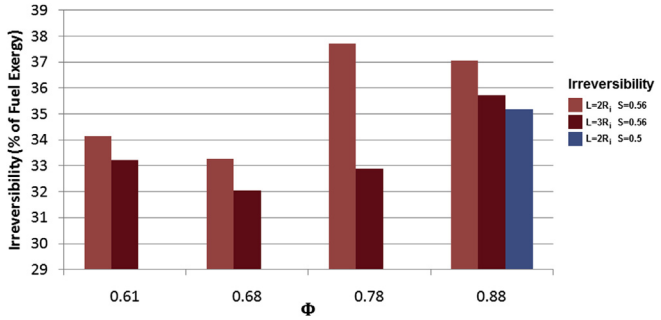

Fig. 10. Comparison of system irreversibility for recess and swirl variation.

rise of the irreversibility ratio for fuel–air mixtures stronger than $\Phi = 0.68$ is mainly governed by the influence of the flame regime on the fuel exergy destruction. As the equivalence ratio increases that accompanies the bulk velocity reduction, the combustion is shifting toward the attached flame regime which has greater potential for the generation of thermal entropy.

Figs. 9 and 10 also reveal the effect of swirl number on the exergy distribution and irreversibility. Apparently, reducing the swirl number improves the exergy performance of the low swirl combustion. It is observed in Fig. 9 that reducing the swirl number from 0.56 to 0.5 (at $L = 2R_i$) enhances the exergy transferred by heat and abates the exergy associated with the exhaust gases. Apparently in Fig. 10, the irreversibility of combustion is meaningfully suppressed relatively 5.4 percent as the burner swirl number is reduced. This fact rises against the observations for ordinary diffusion burners where decreasing the swirl number usually increases the fuel exergy destruction [21,22]. The difference is due to the premixed nature of LSB combustion, which does not depend on swirl-induced recirculation for combustion completion. Therefore, by reducing the swirl number of LSB, the intensity of shear layers would be restricted which leads to reduction of viscous dissipations (Eq. (12)). More importantly, reduction of combustion swirl gives rise to the flame lift-off and promotes lifted flame regime. As a consequence, the lower thermal entropy would be generated due to the inherent feature of lifted flames.

4.2.3. *Effect of thermal input rate*

Low swirl burners benefit from a self-adjusting mechanism by which they can withstand rather a wide range of operating capacity without flameout occurrence. The low swirl burner is investigated in order to evaluate the effect of thermal input rate on the exergy performance of combustion.

As Fig. 11 displays, the exergy associated with heat transfer is primarily improving when the thermal input rate is rising from 36 to 57 kW while the exhaust flow exergy remains nearly unchanged. Meanwhile, the exergy destruction is reduced in this interval due to the improvement of exergy associated with heat and exhaust flow. For the input rates beyond 57 kW, the heat exchange exergy experiences a drop, whereas the exhaust exergy is increasing. This issue is mainly due to the fact that as thermal input rate is increasing, the gases mean residence time gets to a point which yields to less exergy transfer to the walls and more exergy of exhaust gas flow. However, the irreversibility is suppressed by increasing thermal input rate, which is a consequence of better performance of the combustion system. In fact, in higher thermal input rates, the internal irreversibilities are hardly changing while the input exergy is being added that results in lowering the total irreversibility ratio.

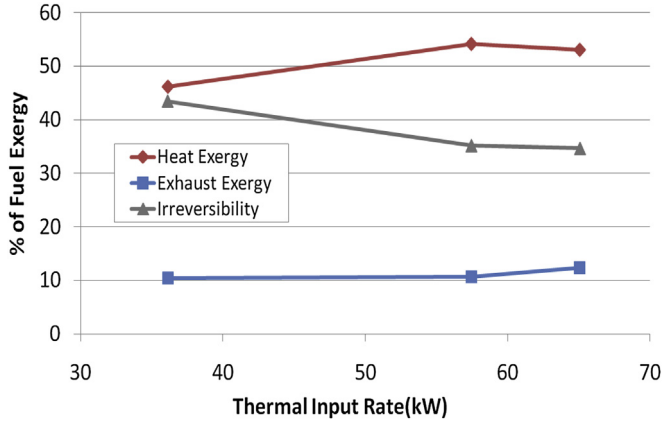

Fig. 11. Effect of thermal input rate on various exergy terms of combustion system ($\Phi = 0.88$, L=2R$_i$, $S = 0.5$).

5. Conclusion

The exergy analysis is carried out on a premixed low swirl burner (LSB) operating on natural gas. The experiments are conducted in a fashion that the effect of design and operating parameters on the exergy distribution of the system can be investigated. The study of the combustion system yields the following outcomes:

- The attached and lifted flames are two dominant regimes that are highly influenced by fuel–air mixture and LSB design characteristics. The attached flame often exhibits more exergy destruction due to the strong temperature gradients outside of the flame.
- The exergy associated with heat transfer from the flame to the combustor walls in the lifted flames is significantly greater than its value in the attached flames. On the other hand, the exergy transfer via the exhaust gases is slightly more in the attached flames in comparison with the lifted flames.
- In the present study, on the average basis, the fuel exergy destruction of the premixed combustion is 34.5%, while this value for ordinary diffusion turbulent flames is usually quite larger.
- When the flame regime shifts from lifted to attached due to Φ variations, the irreversibility ratio experiences almost 13% rise relatively. This issue highlights the advantage of lifted flames in restricting the irreversibility production.
- Increasing LSB recess length from $2R_i$ to $3R_i$ generally increases the exergy associated with heat transfer from the flame to the walls by 14.8% and reduces the combustion irreversibility by 5.6%, relatively. However, the changes of exhaust gas exergy vary independently with L.
- Reducing the swirl number of the present LSB causes improvement in the heat exergy term, while limits the exhaust exergy. As S decreases from 0.56 to 0.5, the irreversibility is suppressed by 5.4% comparatively.
- As the thermal input rate of the burner increases, the irreversibility ratio declines which is probably due to the insensitivity of entropy generation sources to the thermal input rate.

Consequently, the results of this study suggests that within the stability range of LSB combustion, by increasing the recess length and reducing swirl number the fuel exergy destruction will be limited.

Acknowledgment

The authors are grateful for the support provided in the present work by the School of Engineering of the Ferdowsi University of Mashhad and also Kh-Razavi Gas Company.

References

[1] Boyd Fackle K, Karalus MF, Novosselov IV, Kramlich JC, Malte PC. Experimental and numerical study of NO_x formation from the lean premixed combustion of CH_4 mixed with CO_2 and N_2. J Eng Gas Turbines Power 2011;133.
[2] Gokulakrishnan PM, Ramotowski J, Gaines G, Fuller C, Joklik R, Eskin LD, et al. A novel low NO_x lean, premixed, and prevaporized combustion system for liquid fuels. J Eng Gas Turbines Power 2008;130.
[3] Dunn-Rankin D. Lean combustion – technology and control. USA: Academic Press; 2008.
[4] Huang Y, Yang V. Dynamics and stability of lean-premixed swirl-stabilized combustion. Prog Energy Combust Sci 2009;35:293–364.

[5] Syred N, Beer JM. Combustion in swirling flow: a review. Combust Flame 1974;23:143–201.
[6] Chan CK, Lau KS, Chin WK. Freely propagating open premixed turbulent flames stabilized by swirl. In: 23rd Symposium on combustion; 1992. p. 511–8.
[7] Yegian DT, Cheng RK. Development of a lean premixed low-swirl burner for low NO_x practical applications. Combust Sci Technol 1998;139:207–27.
[8] Cheng RK. Velocity and scalar characteristics of premixed turbulent flames stabilized by weak swirl. Combust Flame 1995;101:1–14.
[9] Cheng R, Littlejohn D, Noble DR, Lieuwen T. Laboratory investigations of low-swirl injectors operating with syngases. J Eng Gas Turbines Power ASME 2010;132. 011502-1.
[10] Cheng RK, Littlejohn D, Nazeer WA, Smith KO. Laboratory studies of the flow field characteristics of low-swirl injectors for adaptation to fuel-flexible turbines. J Eng Gas Turbines Power 2008;130.
[11] Johnson MR, Littlejohn D, Nazeer WA, Smith KO, Cheng RK. A comparison of the flowfields and emissions of high-swirl injectors and low-swirl injectors for lean premixed gas turbines. Proc Combust Inst 2004;30(2005): 2867–74.
[12] Cheng RK, Yehian DT, Miyatso MM. Scaling and development of swirl burners for low emission furnace and boilers. Proc Combust Inst 2000;28:1305–13.
[13] Day Marc, Tachibana Shigeru, Bell John, Lijewski Michael, Beckner Vince, Cheng Robert K. A combined computational and experimental characterization of lean premixed turbulent low swirl laboratory flames. Combust Flame 2012;159:275–90.
[14] Wark K. Advanced thermodynamics for engineers. McGraw Hill Inc; 1995.
[15] Arpaci VS, Selamet A. Entropy production in flames. Combust Flame 1998;73: 251–9.
[16] Nag PK. Engineering thermodynamics. Tata McGraw-Hill Education; 2005.
[17] Dunbar WR, Lior N. Sources of combustion irreversibility. Combust Sci Technol 1994;103:41–61.
[18] Nishida K, Takagi T, Kinoshita S. Analysis of entropy generation and exergy loss during combustion. Proc Combust Inst 2002;29:869–74.
[19] Som SK, Datta A. Thermodynamic irreversibilities and exergy balance in combustion processes. Prog Energy Combust Sci 2008;34:351–76.
[20] Stanciu D, Isvoranu D, Marinescu M, Gogus Y. Second law analysis of diffusion flames. Int J Appl Thermodyn 2001;4:1–18.
[21] Yapici H, Kayatas N, Albayrak B, Basturk G. Numerical calculation of local entropy generation in a methane–air burner. J Energy Convers Manag 2005;46:1885–919.
[22] Makhanlall D, Liu L. Entropy production analysis of swirling diffusion combustion processes. Front Energy Power Eng China 2010;4:326–32.
[23] Li J, Chou SK, Yang WM, Li ZW. A numerical study on premixed micro-combustion of CH_4–air mixture: effects of combustor size, geometry and boundary conditions on flame temperature. Chem Eng J 2009;50:213–22.
[24] Regulagadda P, Dincer I, Naterer GF. Exergy analysis of a thermal power plant with measured boiler and turbine losses. Appl Therm Eng 2010;30:970–6.
[25] Hasanuzzaman M, Saidur R, Rahim NA. Energy, exergy and economic analysis of an annealing furnace. Int J Phys Sci 2011;6:1257–66.
[26] Taniguchi H, Mouri K, Nakahara T, Arai N. Exergy analysis on combustion and energy conversion processes. Energy 2005;30:111–7.
[27] Rakopoulos CD, Giakoumis EG. Second-law analyses applied to internal combustion engines operation. Prog Energy Combust Sci 2006;32:2–47.
[28] Incropera FP, DeWitt DP, Bergman TL, Lavine AS. Introduction to heat transfer. Wiley; 2007.
[29] Kotas Tadeusz J. The exergy method of thermal plant analysis. UK: Anchor Brendon; 1985.
[30] Briones AM, Mukhopadhyay A, Aggarwal SK. Analysis of entropy generation in hydrogen-enriched methane–air propagating triple flames. Int J Hydrog Energy 2009;34:1074–83.
[31] Feyz ME, Esfahani JA. Exergetic performance of a cylindrical methane–air microcombustor under various inlet conditions. Int J Exergy 2014;15:257–75.

Nomenclature

ACV: control volume availability/exergy
h: enthalpy
h_{conv}: convection heat transfer coefficient
h_r: radiation heat transfer coefficient
Irr: irreversibility ratio
$\dot{I}_{CV}$: irreversibility
K: coefficient of conduction
L: recess length
m_c: mass flow of central channel
m_a: mass flow of annular channel
$\dot{m}_f$: fuel mass flow rate
$\dot{m}_{air}$: air mass flow rate
Nu: Nusselt
P: static pressure (Pa)
P_0: dead-state pressure (MPa)
Pr: Prandtl
$\dot{Q}_i$: heat transfer rate
R: burner radial ratio
$\overline{R}$: universal gas constant
r_m: mass flow ratio
s_i: entropy of the *i*th species
S: swirl number
T_i: temperature of the *i*th species (K)
T_o: dead-state temperature (K)
T_{sur}: surrounding temperature (K)
u: axial velocity (m s^{-1})
U_0: bulk velocity
V_{cv}: volume of control volume
s: integral surface
V_s: normalized laminar flame speed
W_{cv}: shaft work

Greek symbols

μ: dynamic viscosity (kg m^{-1} s^{-1})
ε: emissivity
σ: Stefan–Boltzmann constant (W m^{-2} K^{-4})
ψ_{in}: inlet flow exergy (kW)
ψ_{out}: outlet flow exergy (kW)
μ_i: chemical potential of the *i*th species
Φ: equivalence ratio
Φ_v: viscous dissipation
ε_i^o: standard chemical exergy of the *i*th species (kW)